

Sine-Liouville gravity as a Vertex Model on Planar Graphs

Ivan Kostov ^{a,b}

^a *Université Paris-Saclay, CNRS, CEA, Institut de physique théorique
91191 Gif-sur-Yvette, France*

^b *Beijing Institute of Mathematical Sciences and Applications
Huairou 101408, Beijing, China*

E-mail: ivan.kostov@ipht.fr

ABSTRACT: We investigate the universal behaviour of a one-parameter generalisation of the six-vertex model on planar graphs, which we refer to as the 7-vertex model (7vM). The 7vM is characterised by a temperature coupling and its continuum limit is characterised by a massive, dilute and dense phases similarly to the $O(n)$ loop model. We compute the sphere and disk partition functions of the 7vM from the spectral curve of the dual matrix model, abbreviated here as 7vMM. The disk partition function for fixed length is expressed in terms of an uncharted deformation of the K-Bessel functions. We argue that 7vMM and Matrix Quantum Mechanics (MQM) provide two complementary non-perturbative realisations of sine-Liouville gravity. Specifically, we find that the continuum limit of 7vMM and the MQM share the same classical spectral curve but describe two different types of branes in sine-Liouville gravity. The 7vMM precisely covers the range of parameters where the Minkowskian MQM lacks a simple interpretation in terms of multiple tachyon scattering. We investigate the flow relating the dilute and the dense phases and argue that this flow is the gravitational analogue of the massless flow in the sine-Gordon model with imaginary mass coupling. The two extremities of the flow are described by a free boson coupled to Liouville gravity and compactified at circles with two different radii.

In memory of Ivan Todorov

Contents

1	Introduction and summary	1
2	Sine-Liouville gravity	5
2.1	Sine-Gordon QFT	5
2.2	Sine-Liouville gravity	7
3	The 7-vertex model on planar graphs	9
3.1	Definition and loop expansion	9
3.2	The 7-vertex matrix model	11
3.3	Collective field and Virasoro constraint	12
4	Thermodynamical limit and spectral curve	14
4.1	Boundary value problem	14
4.2	Phase diagram and continuum limit	15
4.3	Uniformisation of the boundary value problem in the continuum limit	16
4.4	Solution at the critical point ($M = 0$)	18
4.5	Solution of the boundary value problem in the continuum limit	18
4.6	Computation of the boundary entropy	19
4.7	Partition function on the sphere and susceptibility	20
4.8	Boundary length distribution	21
5	Relation to Matrix Quantum Mechanics and 2D string theory	22
5.1	The classical spectral curve of MQM	22
5.2	7vMM versus MQM	24
6	Discussion	26

1 Introduction and summary

Sine-Liouville gravity, or sine-Gordon model coupled to 2D gravity, is a rich and fascinating theory. Although it has been studied for more than three decades, starting with [1, 2], some aspects of the theory, especially concerning the boundary behaviour, are still poorly understood.

The sine-Liouville gravity is closely related to the sine-Liouville CFT which, according to the Fateev-Zamolodchikov-Zamolodchikov (FZZ) conjecture [3, 4] proved rigorously in [5], is mapped by strong/weak coupling duality to the Euclidean black hole (cigar) CFT [6, 7]. A non-perturbative description of the sine-Liouville gravity is given by Matrix Quantum Mechanics (MQM) [8–11] perturbed by a source of winding [12] or momentum [13] modes. The perturbed MQM exhibits Toda integrability, first discovered in [14] and then exploited

to investigate different aspects of the 2D string theory: winding mode [12] and momentum mode [13, 15] condensates, and non-perturbative effects due to sine-Liouville instantons [16, 17].

In this paper we present an alternative holographic dual of Euclidean sine-Liouville gravity with a neat statistical interpretation. Our construction is based on the integrable lattice regularisation of the sine-Gordon quantum field theory provided by a 7-vertex model on a regular hexagonal (honeycomb) lattice. This vertex model, first studied by Baxter [18], gives a local formulation of the $O(n)$ model [19]. The local degrees of freedom of the vertex model are arrows assigned to the bonds of the honeycomb lattice obeying the “ice rule” that the numbers of incoming and outgoing arrows at each site must be equal. The ice rule allows 7 configurations at each vertex of the graph as shown in fig. 1. The local Boltzmann weights are associated with these seven vertex configurations, or simply vertices. Assuming invariance under $\pi/3$ rotations, which we must do when we consider dynamical lattices, there are only 3 distinct vertices which can be parametrised up to a common factor as

$$w_1 = T, \quad w_2 = w_3 = w_4 = w, \quad w_5 = w_6 = w_7 = w^{-1}. \quad (1.1)$$

The parameter T is sometimes referred to as temperature. Each vertex configuration defines a collection of self-avoiding and mutually avoiding oriented loops, and the partition sum of the vertex model is expanded as

$$\mathcal{Z} = T^{\#\text{sites}} \sum_{\text{oriented loops}} T^{-\#\text{[occupied sites]}} w^{\#\text{[left turns]} - \#\text{[right turns]}}. \quad (1.2)$$

Since on the infinite lattice the number of the right turns differ from the number of the left turns by ± 6 , the loop expansion (1.2) is that of the $O(n)$ model with $n = w^6 + w^{-6}$ [19].

The loop gas exhibits nontrivial critical behavior when w is unimodular complex number so that $|n| \leq 2$. Its phase diagram shows two critical phases, the phase of dilute loops at $T_c = (2 + \sqrt{2-n})^{1/2}$ and the critical phase of dense loops at $T < T_c$. The two critical phases correspond to the two renormalisation-group fixed points of the sine-Gordon theory with imaginary coupling constant and the massless flow connecting them was investigated in a series of renown papers by P. Fendley, H. Saleur and Al. Zamolodchikov [20–22].

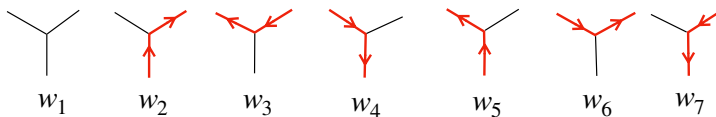


Figure 1. The vertices of the 7-vertex model.

The 7-vertex model can be defined on any trivalent planar graph. Sometimes it is useful to represent the graph by its dual triangulation where we can define local curvature associated with the vertices of the triangulation. An example of a vertex configuration on a trivalent graph with the topology of a disk together with its dual triangulation is shown in fig. 2. Considering the ensemble of all trivalent planar graphs, we add the gravitational

degrees of freedom and arrive at an integrable lattice regularisation of the gravitational sine-Gordon model. Geometrically, the vertex model on planar graphs represents a gas of oriented self and mutually avoiding loops and in this respect resembles the gravitational $O(n)$ loop model [23]. The dynamics is however quite different because the Boltzmann weights of the loops depend on the local curvature through an effective spin connection. In general, vertex models on planar graphs represent a separate and still unexplored niche of solvable models of 2D gravity, and can reveal new unexpected phenomena, especially in case of lattices with boundaries.

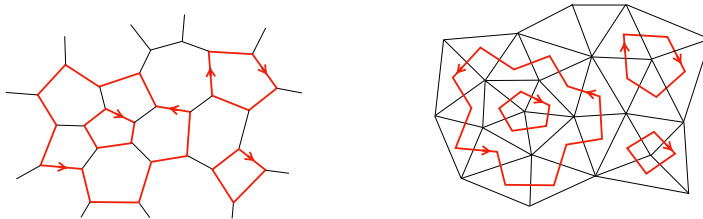


Figure 2. A loop configuration on a trivalent graph with the topology of the disk and on its dual triangulation. To preserve the information about the topology the lines should be thickened.

We solve the gravitation 7-vertex model by mapping it to the large- N limit of an $U(N)$ -invariant matrix model. The matrix model in question is one-parameter generalisation of the 6-vertex matrix model studied in [24–26]. With the volume of the $U(N)$ symmetry group factored out, the partition function of the matrix model is an N -fold integral

$$\mathcal{Z}_N \sim \int_{-\infty}^{\infty} \prod_{i=1}^N dx_i e^{-\frac{1}{\hbar} V(x_i)} \prod_{i \neq j} \frac{x_i - x_j}{q^{1/2} x_i - q^{-1/2} x_j} \quad (1.3)$$

where the dependence on the temperature coupling is encoded in the cubic potential $V(x)$ and the parameter $q = -w^2$. In the large N limit, the integral depends on two adjustable parameters, the temperature T and the lattice cosmological constant $\kappa = \hbar N$. Interesting critical behaviour occurs only if $|q| = 1$. For $q = -1$, this is the partition function of the gravitational $O(2)$ model. We will parametrise the vertices in fig. 1 in a way compatible with the conventions of [25] by setting in (1.1)

$$w = e^{-i\pi\lambda/2}. \quad (1.4)$$

Then for $T = 0$ the integral (1.3) is exactly the partition function of the 6-vertex matrix model. Besides q and λ , we will use at different places the parameters β and b related to the parameter $\lambda \in [0, 1]$ by

$$q = e^{i\beta}, \quad \beta = \pi(1 - \lambda), \quad b = \sqrt{\frac{1 - \lambda}{1 + \lambda}}. \quad (1.5)$$

The full solution of the matrix model will be reported in a forthcoming paper [27]. Here we focus on the universal behaviour in the continuum limit $\kappa \rightarrow \kappa_*$ and $T \rightarrow T_*$ expected to be described by sine-Liouville gravity.

The thermodynamical limit of the matrix model is encoded in its classical spectral curve. Here by spectral curve we understand a complex manifold with punctures and given behavior of the functions on this manifold at the punctures. The matrix model corresponds to a particular real section of this curve coinciding with one of its two non-contractible cycles

We found the following parametric form for the classical spectral curve in the continuum limit,

$$\begin{aligned} x &= M(\omega^b - \omega^{-1/b}), \\ y &= M^{1/b^2} \omega^{1/b} - t M^{b^2} \omega^{-b}. \end{aligned} \tag{1.6}$$

Here $t = T - T_*$ is the renormalised temperature and the renormalised cosmological constant $\mu \sim \kappa - \kappa_*$ enters implicitly through the quantity M ,

$$M^{1+\frac{1}{b^2}} - b^2 t M^{1+b^2} = (1 + b^2)\mu. \tag{1.7}$$

The meromorphic function $y(x)$, which is given in parametric form by eq. (1.6), determines the partition function on the disk with complexified boundary parameter x and eq. (1.7) determines the boundary entropy generated by the fluctuations of the bulk which is proportional to M .

The free energy $\mathcal{F} = \hbar \log \mathcal{Z}$ takes simpler form in the grand canonical ensemble where the bulk cosmological constant μ is conjugated to the size N of the matrix and a sum over N is performed. We find that the boundary entropy M and the susceptibility $u(\mu, t) = \partial_\mu^2 \mathcal{F}$ are related by

$$M = e^{-(1-\lambda)u}, \tag{1.8}$$

which turns (1.7) into a thermodynamical equation of state

$$\mu = \frac{1+\lambda}{2} e^{-\frac{1+\lambda}{2}u} - \frac{1-\lambda}{2} t e^{-\frac{1-\lambda}{2}u}. \tag{1.9}$$

This equation has three critical points $t = 0, t \rightarrow -\infty$ and $t = t_c > 0$ and indeed reflects the phase diagram of the sine-Gordon model on the plane [20–22].

The role of scale parameter in sine-Liouville gravity is played by the cosmological constant μ which determines the size of the two-dimensional universe. The limit of large μ describes the UV limit of the matter field which is that of a free compactified boson. When t becomes large and negative, the effective cosmological constant $-\mu/t$ diminishes and eq. (1.9) explores the physics at large distances. The limit $t \rightarrow -\infty$ thus corresponds to the IR fixed point of the imaginary coupled sine-Gordon model. The third critical point $t = t_c$ is that of pure gravity and corresponds to the massive phase.

We find that at $t = 0$ and $t \rightarrow -\infty$ the matter field is that of a free boson on a circle of radius respectively R_{UV} and R_{IR} related to the parameter λ of the vertex model as

$$R_{\text{UV}}^{\text{SL}} = \frac{1+\lambda}{2}, \quad R_{\text{IR}}^{\text{SL}} = \frac{1-\lambda}{2}. \tag{1.10}$$

In our conventions the self-dual radius is 1. The parameter λ does not renormalise after switching on the gravitational field but the compactification radius does. If we denote by

R_{UV}^{SG} in $R_{\text{IR}}^{\text{SG}}$ the radii at the two RG fixed points of the imaginary coupled sine-Gordon which describe the continuum limit, then

$$2R_{UV}^{\text{SG}} = \sqrt{2R_{UV}^{\text{SL}}}, \quad 2R_{\text{IR}}^{\text{SG}} = \sqrt{2R_{\text{IR}}^{\text{SL}}}. \quad (1.11)$$

More generally, we claim that coupling to gravity changes the radius of compactification. A gaussian field taking values in the circle of radius R_0 , after coupling to gravity will take values in the circle of different radius

$$R_{\text{gravitational}} = 2R_0^2 \quad (1.12)$$

unless $R_0 = R_{\text{BKT}} (= 1/2)$. This relation, which is a variant of the KPZ scaling in 2D gravity [28–30], is not a priori evident, at least for the author. It has been previously observed experimentally in [25] by comparing the solution of the 6-vertex model on flat and random lattices.

As expected, the equation of state (1.9) is the same as the equation of state of MQM [12, 13, 31]. Thus, if restricted to the bulk observables, we have two different non-perturbative realisations of the same world-sheet theory. On the other hand, the boundary observables in the two theories are *different* because the two models are associated with two different Riemann surfaces associated with the same spectral curve. In MQM, the boundary observables are expressed at $t = 0$ and at $t \rightarrow -\infty$ by K -Bessel functions. On the other hand, in 7vMM the boundary observables are expressed in terms of an uncharted deformation of the K -Bessel functions.

The plan of the paper is as follows. We start by reviewing in sect. 2 the phase structure of the sine-Gordon model and sine-Liouville gravity. In sect. 3 we define partition function of the vertex model and derive its representations in terms of a gas of oriented loops on planar graphs and as an interaction-round-a-triangle height model. Then we formulate the dual large- N matrix model and formulate the Dyson-Schwinger equations as Virasoro constraint for a collective bosonic field.

In section 4 we formulate the classical Virasoro constraint as a boundary value problem, obtain the solution at the critical point and in the continuum limit, and derive the partition functions on the sphere and on the disk. For the latter we give expressions both for fixed boundary parameter and for fixed boundary length. In section 5 we explain how the spectral curve of 7vMM compares to that of MQM and the consequences of the new understanding of the phase diagram for the proposal of [12] for a MQM-based description of the Euclidean “cigar” background.

2 Sine-Liouville gravity

2.1 Sine-Gordon QFT

We start with summarising the properties of the sine-Gordon model which we are going to use, such as the phase diagram, with the main purpose of fixing the notations. The sine-Gordon field theory can be thought of as a CFT of a free boson taking values in the

circle of radius $1/2$, i.e. $\varphi + \pi \equiv \varphi$, and perturbed by a pair of exponential fields $e^{\pm 2i\varphi}$,

$$\mathcal{A}_{SG}[\varphi] = \int \frac{g}{4\pi} (\partial_\mu \varphi)^2 + \mu_+ \int d^2x e^{2i\varphi} + \mu_- \int d^2x e^{-2i\varphi}. \quad (2.1)$$

The constant g is usually referred to as Coulomb gas coupling because of the interpretation of the partition function as a gas of positive and negative charges [19]. The Coulomb gas coupling is related to the standard sine-Gordon coupling β_{SG} as $g = 8\pi/\beta_{SG}^2$. In terms of another commonly used parameter p ,

$$g = \frac{p+1}{p}. \quad (2.2)$$

Because of the charge conservation, the bulk observables depend only on the product

$$t = \mu_+ \mu_-. \quad (2.3)$$

We are concerned here only in the regime $1 < g < 2$ where the perturbation in the UV action (2.1) is relevant and the sine-Gordon interaction is repulsive. For real couplings μ_\pm , the renormalisation group (RG) analysis gives [32]

$$\partial_r \mu_\pm = \left(2 - \frac{2}{g}\right) \mu_\pm, \quad \partial_r \log g = 8\pi^2 \mu_+ \mu_- \quad (2.4)$$

where r is the rescaling parameter. By the first equation the couplings constants μ_\pm increase along the RG flow, by the second equation the Coulomb gas coupling g grows, which makes the perturbation even more relevant. The renormalised values of μ_\pm grow faster, the positive and negative charges proliferate, and the sine-Gordon model flows to a trivial massive plasma phase.

On the other hand, if μ_\pm are purely imaginary, their absolute values initially increase under renormalisation according to the first RG equation. However, since their product is negative, and by the second RG equation the Coulomb gas coupling g decreases and the perturbation becomes less relevant. As a result, the Coulomb gas rarifies in the IR and the SG model flows again to a gaussian field, but with smaller value of the coupling constant $g_{IR} < 1$, so that the perturbation becomes irrelevant. The effective central charge starts at $c_{UV} = 1$ in the UV region, oscillates once around this value and returns ultimately again at $c_{IR} = 1$ in the IR [20, 22]. Since for imaginary coupling the theory is not unitary, Zamolodchikov's c -theorem does not apply for this flow.

With the help of the RG equations (2.4), one can determine the coupling constant at the endpoint of the flow in the IR. In the UV, the dimensions of the perturbing operators $e^{\pm 2i\varphi}$ are

$$h = \bar{h} = \frac{1}{g} = \frac{p}{p+1}. \quad (2.5)$$

For small t , the SG perturbation can be considered as triggered by a neutral local operator with coupling constant (2.3) and conformal dimensions

$$h_{SG} = \bar{h}_{SG} = 2h - 1 = \frac{2-g}{g} = \frac{p-1}{p+1}. \quad (2.6)$$

For large p , the two RG equations (2.4) give [19–21]

$$\frac{dg}{dr} = 2 [(g - 1)^2 - 1/p^2]. \quad (2.7)$$

There are two fixed points of this equation, $g^{\text{UV}} = 1 + 1/p$ and $g^{\text{IR}} = 1 - 1/p$.

Instead of the coupling g , one can speak of the compactification radius. Setting $g = (2R)^2$ and rescaling $\varphi \rightarrow \varphi/(2R)$, we have a CFT of a gaussian field with $g = 1$ and taking values in a circle of radius R . The massless RG flow then relates two $c = 1$ CFTs of free boson with different compactification radii¹

$$R_{\text{UV}}^{\text{SG}} = \frac{1}{2}\sqrt{1 + 1/p}, \quad R_{\text{IR}}^{\text{SG}} = \frac{1}{2}\sqrt{1 - 1/p}. \quad (2.8)$$

With this normalisation, the T-duality transforms $R \rightarrow \tilde{R} = 1/R$. When $g = 1$, then $R_{\text{IR}} = R_{\text{UV}} = R_{\text{BKT}} = 1/2$.

There are strong reasons, summarised in [20], to believe that the sine-Gordon model represents the effective quantum field theory describing the vicinity of the critical point T_c for the 7-vertex model, with the constant t proportional to the algebraic distance to critical value, $t \sim T - T_c$. The parameter p of the sine-Gordon interaction is related to the fugacity $n = w^6 + w^{-6}$ of the by $n = 2 \cos(\pi/p)$. One can think of the oriented loops as kinks interpolating between adjacent classical vacua of the sine-Gordon potential. In the massive phase $T > T_c$ ($t > 0$), the theory falls in one of the vacua. Drops of other classical vacua can appear but they are exponentially suppressed. At $T = T_c$ ($t = 0$), the kinks become massless and stay massless for $T < T_c$ ($t < 0$). For large negative t the kinks fill densely the lattice and form a critical phase.

2.2 Sine-Liouville gravity

Now let us consider the sine-Liouville gravity, i.e. a theory of 2D gravity where the sine-Gordon field plays the role of a matter field. This theory, also referred to as gravitational sine-Gordon model, was first studied by G. Moore [1]. In conformal gauge for the gravitational field, the action depends on the sine-Gordon field φ and the scale factor ϕ of the metric known as Liouville field,

$$\begin{aligned} \mathcal{A}_{\text{SL}}[\phi, \varphi] = & \frac{1}{4\pi} \int_{\mathcal{M}} d^2z \sqrt{\hat{g}} \left[(\hat{\nabla}\phi)^2 + (\hat{\nabla}\varphi)^2 + Q\phi\hat{R} \right] + \text{ghosts} \\ & + \mu \int d^2z \sqrt{\hat{g}} e^{2b\phi} + \sum_{\pm} \mu_{\pm} \int d^2z \sqrt{\hat{g}} e^{\alpha\phi} e^{\pm ia\varphi}, \quad a = \frac{1}{R}. \end{aligned} \quad (2.9)$$

¹The IR fixed point has a microscopic realisation as the the 6-vertex model on a square lattice with $\Delta = -2 \cos(\pi/p)$, the compactification radius extracted from the partition function on the torus [19, 33] is that of a Gaussian field taking values in S^1/\mathbb{Z}_2 orbifold [34] of radius $R_{\text{6v}}^{\text{orb}} = 1/\sqrt{1 - 1/p}$ in the convention where $R_{\text{self-dual}} = 1$. The orbifold symmetry is not preserved when the model is defined on a random lattice, and we have to compare instead with the compactification radius for a gaussian field on a circle, which is twice larger, $R_{\text{6v}}^{\text{circ}} = 2R_{\text{6v}}^{\text{orb}}$. Thus $R_{\text{6v}}^{\text{circ}} = 1/R_{\text{IR}}^{\text{SG}}$, which means that the vacuum energy of the vertex model renormalises to the vacuum energy of the T-dual field $\tilde{\varphi}$.

The second line can be considered as perturbation of a gaussian field φ compactified on a circle of length $\beta = 2\pi R$. The exponents should satisfy the marginality condition

$$\frac{1}{4}2b(2Q - 2b) = 1, \quad \frac{1}{4}\alpha(2Q - \alpha) + \frac{1}{4}a^2 = 1. \quad (2.10)$$

In the absence of a background charge for the matter field, the values of Q, b, α obeying (2.10) are determined by the condition that the conformal anomaly vanishes:

$$c_\phi + c_\varphi = 1 + 6Q^2 + 1 = 26 \quad \Rightarrow \quad Q = 2, \quad b = 1, \quad \alpha = 2 - a. \quad (2.11)$$

Again, the path integral depends only on the product $t = \mu_+\mu_-$. A shift $\phi \rightarrow \phi + \log(r^2)$ is compensated by $\mu \rightarrow \mu/r^2$ and $\mu_\pm \rightarrow \mu_\pm/r^\alpha$ with $\alpha = 2 - 1/R$, so that the coupling $t = \mu_+\mu_-$ scales as

$$t \sim \mu^{2-1/R}. \quad (2.12)$$

The sine-Liouville gravity is expected to describe the universal behaviour of the 7-vertex model on planar graphs. The phase diagram of the gravitational sine-Gordon model must be qualitatively the same as that of the sine-Gordon model in the plane. In particular, the massless flow in the imaginary coupled sine-Gordon model must have its counterpart in the sine-Liouville gravity. We will refer to it abusively as gravitational massless flow.

As we mentioned in the Introduction, the compactification radii characterising the free boson at the two extremities of the flow will be modified by the fluctuations of the gravitational field. To see that, first we first notice that we cannot measure directly the radius but we can measure the dimension of the corresponding exponential field. Then we proceed with a KPZ-DDK-like argument. On the flat surface, the integrated interaction term in (2.1) scales as $[\text{Area}]^{2-g}$ with $g = (2R_{\text{UV}}^{\text{SG}})^2 = 1 + 1/p$. After switching on the gravitational field, the interaction term in (2.9) scales as $\mu^{-\alpha} \sim [\text{Area}]^{(2-1/R)/2}$. The exponents coincide if $2R = (2R^{\text{SG}})^2 = 1 + 1/p$. Hence the compactification radii at two extremities of the massless flow in sine-Liouville gravity are

$$R_{\text{UV}}^{\text{SL}} = \frac{1}{2}(2R_{\text{UV}}^{\text{SG}})^2 = \frac{1 + 1/p}{2}, \quad R_{\text{IR}}^{\text{SL}} = \frac{1}{2}(2R_{\text{IR}}^{\text{SG}})^2 = \frac{1 - 1/p}{2}. \quad (2.13)$$

The relation (2.13) is confirmed by the exact solution of the vertex model coupled to gravity.

We refer to the CFT defined by (2.9)-(2.11) as *sine-Liouville quantum gravity* in order to distinguish it from the *sine-Liouville conformal field theory*. In the latter there is no ghost sector, no Liouville potential, and the condition of vanishing of the total conformal anomaly in (2.10) is replaced by $Q = 1/\alpha$. The marginality of the sine-Liouville perturbation for this background charge is equivalent to the constraint $a^2 - \alpha^2 = 2$. If we ignore the ghost sector, then the sine-Liouville CFT and sine-Liouville QG intersect at $R = 2/3$ and $\mu = 0$.

The FZZ conjecture [3, 4] states that the sine-Liouville CFT is related by strong/weak coupling duality to the ‘‘cigar’’ CFT with central charge $\frac{3k}{k-2} - 1$ [6, 7]. The mapping of the parameters is $a = \sqrt{k}$, $\alpha = 1/Q = \sqrt{k-2}$.

3 The 7-vertex model on planar graphs

3.1 Definition and loop expansion

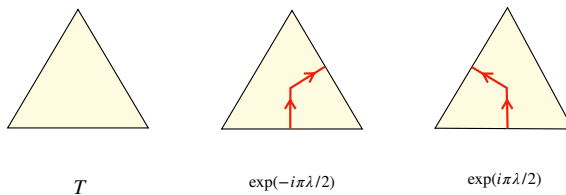
In the 7-vertex model coupled to discrete gravity, the path integral for the gravitational field is discretised as a sum in the ensemble of trivalent planar graphs. For any such graph, the vertex degrees of freedom are introduced by assigning orientations to some of the bonds in such a way that the number of the incoming and the outgoing arrows at each vertex is zero. An example of an allowed vertex configuration is given in fig. 2. Each vertex configuration defines a collection of self- and mutually avoiding oriented loops covering some of the bonds of the graph. In this way the partition function of the vertex model on the sphere can be formulated as that of a gas of oriented loops on trivalent planar graphs,

$$\mathcal{F}_0(\kappa, T) = \sum_{\text{trivalent planar graphs } \mathcal{G}} \kappa^{V_{\mathcal{G}}} \sum_{\text{loops } \mathcal{L} \text{ on } \mathcal{G}} T^{-V_{\text{loops}}} \prod_{\mathcal{L}} e^{i\frac{\pi}{2}\lambda(\#\text{left turns} - \#\text{right turns})} \quad (3.1)$$

where the parameter κ controls the volume $V_{\mathcal{G}}$ (= the total number of vertices of the graph \mathcal{G}) and the temperature T controls the volume V_{loops} occupied by loops (= the number of the vertices of \mathcal{G} visited by loops).

To understand the meaning of the last factor, we can think of a graph \mathcal{G} as the dual object to a triangulation of the sphere by identical triangles, as in fig. 2, right. This can be done in more than one way depending on the chosen form of the triangles from which the triangulation is built. The triangles can have edges of different length but only edges of the same length can be glued together.

The most symmetric choice is that of equilateral triangles with angles $\pi/3$ associated with their vertices. With this choice, for a flat triangulation, there must be exactly 6 triangles meeting at each vertex. If the number of triangles is different, the vertex hosts a conical curvature defect, with the curvature given by the missing angle. There are three distinct types of triangles: the empty triangle with Boltzmann weight T and the triangles visited by a loop turning to the left or to the right with Boltzmann weights $e^{\pm i\pi\lambda/2}$:

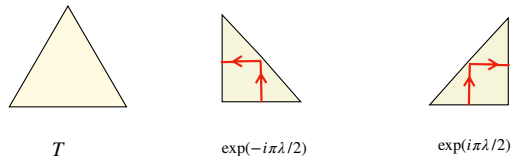


Each vertex configuration describes a set of closed paths \mathcal{L} traversing the edges of the triangulation at right angle and making left or right turns while visiting the triangles. Since the triangles are assumed flat, we can associate an angle $\pm 2\pi/3$ with each turn. Then the product of the weights of the vertices along the path can be interpreted as a holonomy factor generated by parallelly transporting a spinor along the loop. With each left/right turn we associate an elementary holonomy $e^{\pm i\pi\lambda/2}$, i.e. the lattice spin connection for a particle of spin $S = \pi\lambda/3$. Since the local degrees of freedom are defined on the links, the

lattice spin connection is defined on pairs of adjacent links. The phase of the holonomy factor, known also as Berry phase, is the total angle swept of the normal vector.

On a flat lattice the Berry phase is topological and the gas of oriented loops can be identified with the loop expansion of the $O(n)$ model where each loop is weighted by $n = 2 \cos(3\pi\lambda)$. This is no more the case in presence of curvature defects where the holonomy depends on the form of the path \mathcal{L} and on the local curvature. The Berry phase then contains a non-topological piece proportional to the integrated gaussian curvature in the simply connected domain delimited by the loop \mathcal{L} . The $O(n)$ model and the vertex model have different loop expansions and different free energy densities when considered on dynamical triangulations.

The interpretation of the local curvature above is not the only possible one. Another choice for the geometry of the triangular tiles is that they are isosceles triangles with one angle $\pi/2$ and two angles $\pi/4$,



By construction, the arrows are not allowed to cross the longer side. With this choice, in the loop expansion, each segment of a loop represents a left/right turn at $\pm\pi/2$. The flat lattice for equilateral choice now has conical defects whose distribution depend on the vertex configuration.

The vertex model can be mapped to a *height model*. Each vertex configuration determines, up to a constant, an integer-valued height function, with heights assigned to the faces of the trivalent graph. The oriented loops of the corresponding loop configuration divide the planar graph into domains of constant heights, with the oriented loops appearing as domain boundaries. Since the difference of the heights of two neighbouring domains is ± 1 , all the heights but one can be reconstructed from the orientations of the loops. In this way the vertex model can be reformulated as a SOS type height model. The local degrees of freedom of the SOS model are integer-valued heights h_i assigned to the vertices i of the dual triangular lattice. The Boltzmann weight of a height configuration is a product of local factors associated with the elementary triangles Δ_{ijk} ,

$$W_{\Delta}(h_1, h_2, h_3) = \delta_{h_1 h_2} h_{h_2 h_3} A_{h_3 h_1} e^{i\pi\lambda(h_3 - h_1)} + T \delta_{h_1 h_2} \delta_{h_2 h_3} \delta_{h_3 h_1} + \text{cyclic}. \quad (3.2)$$

Here $A_{ab} = \delta_{a, b+1} + \delta_{a, b-1}$ is the adjacency matrix of the A_{∞} Dynkin graph. Expanding the product of the Boltzmann weights in monomials, one obtains exactly the same loop expansion as that of the 7-vertex model.

3.2 The 7-vertex matrix model

The sum over planar graphs decorated by vertices is generated by the perturbative expansion of the following matrix integral which we refer to as 7-vertex matrix model (7vMM),

$$\begin{aligned} \mathcal{Z}_N &= \int d\mathbf{X} d\mathbf{Z} d\mathbf{Z}^\dagger e^{-\frac{1}{\hbar}\mathcal{S}}, \\ \mathcal{S} &= \text{Tr} \left(\frac{1}{2}\mathbf{X}^2 + \mathbf{Z}\mathbf{Z}^\dagger - \frac{T}{3}\mathbf{X}^3 - iq^{1/2}\mathbf{X}\mathbf{Z}\mathbf{Z}^\dagger + iq^{-1/2}\mathbf{X}\mathbf{Z}^\dagger\mathbf{Z} \right), \quad q = e^{i\pi(1-\lambda)}. \end{aligned} \quad (3.3)$$

The integration variables \mathbf{X} and \mathbf{Z} are respectively hermitian and complex $N \times N$ matrices with flat integration measure

$$d\mathbf{X} d\mathbf{Z} d\mathbf{Z}^\dagger = \prod_{i,j} dX_{ij} dZ_{ij} d\bar{Z}_{ij}. \quad (3.4)$$

With the non-perturbative effects neglected, the free energy of the 7-vertex matrix model is a sum over all connected planar (i.e. with thickened lines) Feynman graphs with vertices as in fig. 1. The topology of the planar graphs is controlled by the Planck constant $\hbar \sim 1/N$, and the asymptotic semiclassical expansion is also topological expansion,

$$\hbar^2 \log \mathcal{Z}_N = \sum_{g \geq 0} \hbar^{2g} \mathcal{F}_g(\kappa, \lambda), \quad \kappa = \hbar N, \quad (3.5)$$

with $\mathcal{F}_g(\kappa, \lambda)$ being the partition function of the vertex model in the ensemble of trivalent planar graphs with g handles.

The gaussian integral over the complex matrix can be done explicitly, leaving an $\mathbf{SU}(N)$ -invariant integral over the hermitian matrix \mathbf{X} which reduces to an N -fold integral with respect to the real eigenvalues x_1, \dots, x_N ,

$$\mathcal{Z}_N \sim \int_{-\infty}^{\infty} \prod_{j=1}^N dx_j e^{-\frac{1}{\hbar}(\frac{1}{2}x_j^2 - \frac{T}{3}x_j^3)} \prod_{k \neq j} \frac{x_k - x_j}{1 - iq^{-1/2}x_i + iq^{1/2}x_j}. \quad (3.6)$$

With a shift in the integration variable, the eigenvalue integral takes the form (1.3). For $T = 0$, this is the eigenvalue integral for the 6-vertex matrix model [25].²

The integrand in (1.3) is an $N \times N$ determinant and can be formulated as the partition function of a system of N fermions. In view of comparing with the MQM approach to sine-Liouville gravity [13], it is more convenient to work in the grand ensemble defined as

$$\mathcal{Z}(\mu) = \sum_{N=1}^{\infty} e^{-N\mu/\hbar} \mathcal{Z}_N. \quad (3.7)$$

²Integrals of this type have appeared previously in different contexts: relativistic membranes [35], dimensional reduction of SYM [36, 37], Euclidean black hole [12], Leigh-Strassler deformations of supersymmetric gauge theories [38, 39], and more recently, with non-polynomial potential, as matrix models for topological strings on Calabi-Yau threefolds [40, 41]. Combinatorial aspects of the planar graph expansion of the model (3.3) were addressed in [42].

This is also the formulation which possesses Toda integrability. The grand partition function is a Fredholm determinant

$$\mathcal{Z}(\mu) = \det(1 + K), \quad K(x, x') \equiv \frac{e^{-\frac{\mu + V(x)}{i\hbar}}}{q^{-1/2}x - q^{1/2}x'}, \quad (3.8)$$

with the Fredholm kernel defined with flat integration measure dx on the real axis. The Fredholm determinant describes the grand ensemble of free fermions with fixed Fermi energy μ .

To compute the genus-zero free energy \mathcal{F}_0 , we take the thermodynamical limit $\hbar \rightarrow 0, \mu \rightarrow \infty$ with $\mu\hbar$ fixed. Then the sum in (3.7) is saturated by the saddle-point

$$\partial_\kappa \mathcal{F}_0 = \mu \quad (3.9)$$

with $\kappa = N\hbar$. In the grand ensemble the cosmological constant is identified as the chemical potential μ and the grand partition function is related to the canonical one by Legendre transformation

$$\tilde{\mathcal{F}}_0(\mu) = -\mu\kappa + \mathcal{F}_0(\kappa). \quad (3.10)$$

The basic observable, which serves as a building block for most of the observables, is the L -th moment of the matrix \mathbf{X} ,

$$W_L = \hbar \langle \text{Tr}(\mathbf{X}^L) \rangle_\mu, \quad (3.11)$$

where the expectation value of the trace in the grand ensemble (3.7) is defined as the sum, with a weight $e^{-\mu N/\hbar}$, of the unnormalised expectation values in the sectors with N eigenvalues. The reslvent of the random matrix

$$W(x) = \sum_{L=0}^{\infty} x^{-L-1} W_L = \hbar \left\langle \text{Tr} \frac{1}{x - \mathbf{X}} \right\rangle_\mu \quad (3.12)$$

gives the disk amplitude $W(x)$ with marked boundary and (complexified) boundary constant x .

3.3 Collective field and Virasoro constraint

The grand partition function (3.7) has the form of a Coulomb gas and can be formulated in terms of a collective bosonic field with mode expansion

$$\varphi(x) = \varphi_0 + \alpha_0 \log x - \sum_{n \neq 0} \frac{x^{-n}}{n} \alpha_n, \quad [\alpha_n, \alpha_m] = n \delta_{m+n,0}, \quad [\varphi_0, \alpha_0] = 1. \quad (3.13)$$

The Hilbert space is built on the Fock vacua defined by $\langle 0 | \alpha_{-n} = \langle 0 | \varphi_0 = 0$ and $\alpha_n | 0 \rangle = \alpha_0 | 0 \rangle = 0$ for $n \geq 1$, and the two-point function is

$$\langle 0 | \varphi(x) \varphi(x') | 0 \rangle = \log(x - x'). \quad (3.14)$$

To generate the pairwise interaction of the eigenvalues, which is that of dipoles composed of a positive charge at $q^{1/2}x_j$ and a negative charge at $q^{-1/2}x_j$, we must introduce two more bosonic fields constructed with the same set of oscillators,

$$\begin{aligned}\mathbf{S}(x) &= \frac{\varphi(q^{1/2}x) - \varphi(q^{-1/2}x)}{i}, \\ \varphi(x) &= \alpha_0 \log x + \frac{\Omega(q^{1/2}x) - \Omega(q^{-1/2}x)}{i}.\end{aligned}\tag{3.15}$$

The field $\mathbf{S}(x)$ generates the Coulomb interaction of the eigenvalues and the dual field $\Omega(x)$ creates the external potential. It follows directly from the definition (3.15) that the correlation function of these two fields is

$$\langle 0|\Omega(x)\mathbf{S}(x')|0\rangle = \log(x - x').\tag{3.16}$$

The grand partition function (3.7) then takes the form of a Fock space expectation value

$$\begin{aligned}\mathcal{Z}(\mu) &:= \langle 0|\mathbf{U}_-\mathbf{U}_+|0\rangle, \\ \mathbf{U}_- &:= \exp\left(-\frac{1}{2\pi i\hbar} \oint_{\infty} (\mu + V(x))d\Omega(x)\right), \\ \mathbf{U}_+ &:= \exp\left(\int_{\mathbb{R}} dx : e^{-\mathbf{S}(x)} :\right)\end{aligned}\tag{3.17}$$

with the normal order defined so that the operators α_n with $n \geq 0$ are on the right. The series expansion (3.7) is obtained by expanding the exponential in the right term and using the operator product expansions

$$\begin{aligned}\Omega(x) : e^{-\mathbf{S}(x')} : &\sim \log(x - x') : e^{-\mathbf{S}(x')} : \\ : e^{-\mathbf{S}(x)} : : e^{-\mathbf{S}(x')} : &\sim \frac{(x - x')^2}{(x - q^{-1}x')(x - qx')} : e^{-\mathbf{S}(x)} e^{-\mathbf{S}(x')} : .\end{aligned}\tag{3.18}$$

The observables in the matrix model are represented by operators \mathbf{O} constructed from the oscillator modes with expectation values defined as

$$\langle \mathbf{O} \rangle = \mathcal{Z}(\mu)^{-1} \langle 0|\mathbf{U}_-\mathbf{O}\mathbf{U}_+|0\rangle.\tag{3.19}$$

We normalise the expectation values so that in the limit $\hbar \rightarrow 0$ they remain finite: $S(x) \equiv \hbar \langle \mathbf{S}(x) \rangle$, etc. The expectation value of $\mathbf{S}(x)$ consists of a polynomial piece $S_{\infty}(x) = V(x) + \mu$ and a piece regular at infinity:

$$S(x) \equiv \hbar \langle \mathbf{S}(x) \rangle = S_{\infty}(x) + O(1/x), \quad S_{\infty}(x) = V(x) + \mu.\tag{3.20}$$

Similarly for φ and Ω , with φ_{∞} and Ω_{∞} determined by the defining relations (3.15), and for the currents

$$\mathbf{H}(x) = \partial\mathbf{S}(x), \quad \mathbf{Y}(x) = \partial\varphi(x), \quad \mathbf{J}(x) = \partial\Omega(x).\tag{3.21}$$

The basic observable (3.12) is given by the regular at infinity piece of the expectation value of the current $\mathbf{J}(x)$:

$$W(x) = \hbar \langle \mathbf{J}(x) \rangle - J_\infty(x). \quad (3.22)$$

The dependence of the partition function on μ is through the expectation values of the oscillators φ_0 and α_0 ,

$$\frac{\partial \log \mathcal{Z}(\mu, V)}{\partial \mu} = \frac{\langle \varphi_0 \rangle}{\hbar} \quad \mu = \hbar \langle \alpha_0 \rangle. \quad (3.23)$$

The free energy of the matrix model can be obtained with the help of a conformal Ward identity for the collective field, often referred to as Virasoro constraint, which follows from the OPE

$$: \mathbf{H}(x)^2 : : e^{-\mathbf{S}(x')} : \sim \partial_{x'} \left(\frac{1}{x-x'} : e^{-\mathbf{S}(x')} : \right) + \text{regular}. \quad (3.24)$$

The total derivative form of the rhs assures that the the operator $: \mathbf{H}^2(x) :$ commutes, up to exponentially vanishing boundary terms, with the operator \mathbf{U}_+ in (3.17). Hence for any operator \mathbf{O}

$$\oint_c \frac{dx'}{x-x'} \langle \mathbf{O} : \mathbf{H}(x')^2 : \rangle = 0, \quad (3.25)$$

where the integration contour encloses the real axis and leaves outside all other singularities of the integrand, including the point x . The Virasoro constraint (3.25) is equivalent to the statement that the integrand is analytic in the vicinity of the real axis. The conformal Ward identity (3.25) can also be formulated in terms of the current $\mathbf{Y}(x)$, as the statement that for any operator \mathbf{O} ,

$$\langle \mathbf{O} \cdot \mathbf{Y}(q^{1/2}x) \mathbf{Y}(q^{-1/2}x) \rangle \text{ is analytic in the vicinity of the real axis.} \quad (3.26)$$

Of course, the Virasoro constraint can be as well obtained directly for the matrix integral as a Dyson-Schwinger equation reflecting translation invariance of the measure. The Ward identities (3.25) or (3.26) can be used to reconstruct the whole genus expansion of the free energy. Here we are focusing on the observables on the disk and on the sphere and will take the semiclassical, or thermodynamical, limit $\hbar \rightarrow 0$ where the expectation values of traces factorise and the Virasoro constraint becomes quadratic functional equation for a c-function.

4 Thermodynamical limit and spectral curve

4.1 Boundary value problem

In the limit $\hbar \rightarrow 0$, the fluctuations of the collective field are suppressed and the basic observables are determined completely by the saddle-point spectral density $\rho(x)$ or, equivalently, by the resolvent

$$W(x) = \hbar \left\langle \text{Tr} \frac{1}{x - \mathbf{X}} \right\rangle = \int_{\mathbb{R}} \frac{dx' \rho(x')}{x - x'} \quad (4.1)$$

which by definition is analytic in the x -plane with a cut on some interval $[-a, -b]$ with $a > b > 0$. The expectation values of the three currents,

$$\begin{aligned} J(x) &= \partial\Omega(x) = W(x) + J_\infty(x), \\ Y(x) &= \partial\varphi(x) = \frac{q^{1/2}W(q^{1/2}x) - q^{-1/2}W(q^{-1/2}x)}{i} + Y_\infty(x), \\ H(x) &= \partial S(x) = 2W(x) - qW(qx) - q^{-1}W(q^{-1}x) + H_\infty(x), \end{aligned} \quad (4.2)$$

have respectively one, two and three cuts on rays obtained by rotating the real axis.

As the resolvent $W(x)$ itself does not have simple form even in the continuum limit, it is more convenient to formulate the observables in terms of $Y(x)$. The expectation value $y = Y(x)$ in the thermodynamical limit can be thought of as a projection of a complex curve which we refer to as the classical spectral curve of the matrix model without trying to give it a rigorous definition. The classical spectral curve is determined uniquely by the classical Virasoro constraint (3.26), which is equivalent to the boundary value problem

$$q^{1/2}Y(q^{1/2}e^{\mp i\epsilon}x) = q^{-1/2}Y(q^{-1/2}e^{\pm i\epsilon}x), \quad x \in \text{supp}[\rho]. \quad (4.3)$$

By introducing an elliptic uniformisation map to resolve the four branch points, eq. (4.3) can be transformed into a quasi-periodicity condition on one of the main cycles of the parametrisation torus while on the other cycle it remains periodic. Once the function $Y(x)$ is known, the classical resolvent $W(x)$ is completely determined by the relations (4.2).

In terms of the spectral curve, the two equations eqs. (3.23) can be formulated as integrals around the main cycles of the torus:

$$\partial_\mu \mathcal{F}_0 = -\frac{1}{2\pi i} \oint_{\mathcal{C}_A} Y dx, \quad \mu = \frac{1}{2\pi} \int_{\mathcal{C}_B} Y dx, \quad (4.4)$$

where the contour \mathcal{C}_A encloses the upper cut of $Y(x)$ and the contour \mathcal{C}_B goes from the upper edge of the lower cut to the lower edge of the upper cut.

To express the spectral density itself in terms of $Y(x)$, we write the second relation (4.2) as

$$W(x) = iq^{1/2}Y(q^{1/2}x) + e^{i\beta}W(qx) + \text{polynomial in } x. \quad (4.5)$$

Since $W(x)$ is, by definition, a real analytic function, only the first term in the r.h.s. has a cut $[-a, -b] \subset \mathbb{R}$. The discontinuity of $W(x)$ across this cut is therefore that of the first term, and equal to twice its imaginary part,

$$\rho(x) \equiv \frac{W(x-i0) - W(x+i0)}{2\pi i} = \frac{q^{1/2}Y(q^{1/2}e^{-i\epsilon}x) + q^{1/2}Y(q^{1/2}e^{i\epsilon}x)}{2\pi}. \quad (4.6)$$

4.2 Phase diagram and continuum limit

Obviously the canonical and the grand canonical ensembles exhibit the same critical regimes. The analysis is more straightforward in the canonical ensemble (fixed κ) where the phase diagram is drawn in the (κ, t) -plane.

For $\lambda = 0$, the 7-vertex model is identical to the $O(n)$ loop model with $n = 2$. For $\lambda > 0$, although the vertex model and the $O(n)$ model have different free energies when coupled to gravity, their phase diagrams are expected to be qualitatively the same.

The matrix model is defined classically in a domain in the (κ, t) -space bordered by the critical line where the partition sum is dominated by planar graphs of divergent size. The continuum limit concerns the vicinity of the critical lines and can be achieved both in κ and T directions. When κ increases with T fixed, at some critical value $\kappa = \kappa_c(T)$ the sum over planar graphs diverges because the entropy grows exponentially with the size of the graph. On the other hand, if we keep κ constant and decrease the temperature, below some $T = T_c(\kappa)$ the effective tension of the loops will become negative and the planar graph will be densely filled with loops. The effective bare cosmological constant will be $\kappa_1 = \kappa/T$. Thus, the critical line has two analytic branches which describe two different critical phases, $\kappa = \kappa_c(T)$ (massive loops) and $T = T_c(\kappa)$ (dense loops). The critical point (κ_*, T_*) is at the intersection of the two branches where both the total length of the loops and the volume non-occupied by loops diverge.

In the grand ensemble, the critical point is at (μ_*, t_*) with μ_* related to κ_* by (3.9). The continuum limit concerns the blown-up vicinity of the critical point in the double scaling limit parametrised by the renormalised coupling constants

$$x \rightarrow \epsilon x, \quad \mu - \mu_* \rightarrow \epsilon^{2/(1-\lambda)} \mu, \quad T - T_* \rightarrow \epsilon^{4\lambda/(1-\lambda^2)} t, \quad \epsilon \rightarrow 0. \quad (4.7)$$

where we anticipated the critical indices obtained from the analytic solution we are going to derive below. The observables in the limit $\epsilon \rightarrow 0$ will contain scaling functions of the dimensionless combinations $\hat{t} \sim t/\mu^{2\lambda/(1+\lambda)}$ and $\hat{x} \sim x/\mu^{(1-\lambda)/2}$. The dense critical phase $t \rightarrow -\infty$ is characterised with another set of exponents.

4.3 Uniformisation of the boundary value problem in the continuum limit

The exact solution of the boundary value problem will be reported in a future publication [27]. Here we are only interested in the continuum limit when the parametrisation torus degenerates into a cylinder, with the large cycle defining an UV cutoff.

The continuum limit is achieved by taking $b/a \rightarrow 0$ and simultaneously rescaling x so that the right branch point stays at a finite distance M_b from the origin while the left branch point escapes to infinity. From now on by x we will understand the rescaled variable x . The analytic properties of the function $y = Y(x)$ change accordingly. In the continuum limit, the Riemann surface of $Y(x)$ has two semi-infinite cuts in the main sheet starting at $q^{\pm 1} M_b$ and ending at infinity in the lower/upper semi-plane x (fig. 3, left). Such analytic structure results in having two infinite points, $\Re x \rightarrow +\infty$ and $\Re x \rightarrow -\infty$. One can imagine the Riemann surface as an infinite cover of a sphere with singularities at the north and at the south poles. At the two singular points, the function $Y(x)$ has two different expansions in fractional powers of $1/x$, convergent respectively in the domains \mathbb{C}_+ and \mathbb{C}_- delimited by the two cuts and presented in fig. 3 in yellow and green.

The two cuts are resolved by a uniformisation map $s \rightarrow x$ such that the main sheet of the Riemann surface of $Y(x)$ is parametrised by a strip of width π in the s -plane (fig. 3,

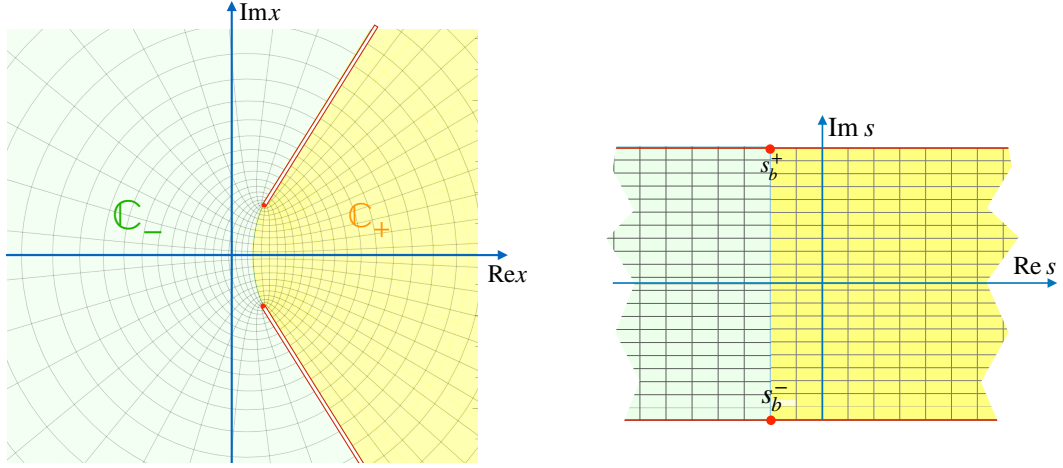


Figure 3. The domains \mathbb{C}_+ and \mathbb{C}_- of the principal sheet of the Riemann surface of $Y(x)$ (left) and in the principal strip of the s -parametrisation plane (right)

right)

$$x(s) = 2M e^{-\lambda s} \sinh s, \quad s \in \mathbb{R} \times [-\frac{1}{2}i\pi, \frac{1}{2}i\pi]. \quad (4.8)$$

The whole Riemann surface is parametrised by extending the map (4.8) to $s \in \mathbb{C}$. The upper and the lower cut are the images of the upper and the lower edge of the parametrisation strip and the pre-images of the two singular points are at $\Re s \rightarrow \pm\infty$.

The parameter M determines the positions of the branch points where $x'(s) = 0$. Besides the two simple branch points in the main sheet there is an infinite number of simple branch points in the lower sheets whose parameters form a vertical array $s_b + 2\pi i(n + 1/2)$ with $n \in \mathbb{Z}$ and

$$s_b = \log b < 0 \quad (b^2 = \frac{1-\lambda}{1+\lambda}). \quad (4.9)$$

The two branch points x_b^\pm in the first sheet are

$$x_b^\pm = x(s_b \pm i\pi/2) = -q^{\pm 1/2} M_b, \quad (4.10)$$

with

$$M_b = (1 + b^{-2}) b^{\frac{2}{1+b^2}} M. \quad (4.11)$$

The domain \mathbb{C}_+ is parametrised by the semi-infinite strip $|\Im s| < \pi/2$, $\Re s > s_b$ and the complementary domain \mathbb{C}_- is parametrised by the half-strip $|\Im s| < \pi/2$, $\Re s < s_b$, as depicted in fig. 3, right.

The uniformisation map (4.8) transforms the boundary value problem into a monodromy problem. The sewing condition (4.3) for $Y(x)$ can be formulated as a quasi-periodicity condition for the functions $x(s)$ and $y(s) = Y[x(s)]$,

$$\begin{aligned} x(s \pm i\pi/2) &= e^{\pm i\beta} x(s \mp i\pi/2), \\ y(s \pm i\pi/2) &= e^{\mp i\beta} y(s \mp i\pi/2). \end{aligned} \quad (4.12)$$

4.4 Solution at the critical point ($M = 0$)

The quasiperiodicity condition (4.12) has infinitely many solutions with different asymptotic behaviour at $x \rightarrow \pm\infty$. In order to be able to recognise the solution relevant for our problem, let us first consider the critical point where $M_b \rightarrow 0$. At the critical point, the bridge connecting the two domains \mathbb{C}_+ and \mathbb{C}_- disappears and the solution has to be looked for separately in each of them,

$$\begin{aligned} \mathbb{C}_- : \quad Y(e^{i\beta}x) &= e^{-i\beta}Y(x) &\Rightarrow Y(x) &\sim (-x)^{\frac{2n}{1+\lambda}-1}, \\ \mathbb{C}_+ : \quad Y(e^{i(2\pi-\beta)}x) &= e^{-i(2\pi-\beta)}Y(x) &\Rightarrow Y(x) &\sim x^{\frac{2n}{1-\lambda}-1}. \end{aligned} \quad (4.13)$$

The integer n should be positive because the density must vanish at the origin. The most general solution for the resolvent is therefore

$$W(x) = \sum_{n \geq 1} t_n^+ \frac{x^{\frac{2n}{1-\lambda}-1}}{2 \sin(\pi n/b^2)} - \sum_{n \geq 1} t_n^- \frac{(-x)^{\frac{2n}{1+\lambda}-1}}{2 \sin(\pi n b^2)}. \quad (4.14)$$

Indeed, from the second relation (4.2) we obtain

$$Y(x) = \begin{cases} -\sum_{n \geq 1} t_n^- (-x)^{\frac{2n}{1+\lambda}-1} & \text{if } x \in \mathbb{C}_-, \\ \sum_{n \geq 1} t_n^+ x^{\frac{2n}{1-\lambda}-1} & \text{if } x \in \mathbb{C}_+. \end{cases} \quad (4.15)$$

This is the most general form of the solution at the critical point.

In our case, the solution is a combination of the two lowest powers,

$$Y(x) = \begin{cases} -t (-x)^{\frac{1-\lambda}{1+\lambda}} & \text{if } x \in \mathbb{C}_-, \\ x^{\frac{1+\lambda}{1-\lambda}} & \text{if } x \in \mathbb{C}_+, \end{cases} \quad (4.16)$$

where we rescaled x to have $t_1^+ = 1$, $t_1^- = t$. Taking the discontinuity of the resolvent (4.14), one finds for the critical spectral density

$$\rho(x) = \frac{|x|^{\frac{1}{b^2}} + t|x|^{b^2}}{2\pi}, \quad x < 0, \quad (4.17)$$

with b defined by (1.5). The rhs of (4.16) determines the large- x asymptotics of the solution in the continuum limit we are looking for.

4.5 Solution of the boundary value problem in the continuum limit

The unique solution of the quasi-periodicity condition (4.12) with large- x asymptotics (4.16) is

$$\begin{aligned} x(s) &= 2M e^{-\lambda s} \sinh s, \\ y(s) &= e^{(1+\lambda)s} M^{\frac{1+\lambda}{1-\lambda}} - t e^{-(1-\lambda)s} M^{\frac{1-\lambda}{1+\lambda}}. \end{aligned} \quad (4.18)$$

With a change of the parameter $s \rightarrow \omega = e^{-2s/(b+b^{-1})}$, this solution takes the form (1.6) announced in the Introduction. The function $y = Y(x)$ is determined in the domains \mathbb{C}_\pm by two different power series whose positive parts are given in our case by (4.15).

The spectral curve in the continuum limit matching the general solution (4.16) has parametric form

$$\begin{aligned} x(s) &= M e^{(1-\lambda)s} - M^{-(1+\lambda)s}, \\ y(s) &= \sum_{n \geq 1} \left(t_n^+ M^{\frac{2n}{1-\lambda}-1} e^{(2n+\lambda)s} - t_n^- M^{\frac{2n}{1+\lambda}-1} e^{-(2n-\lambda)s} \right). \end{aligned} \quad (4.19)$$

For a finite number of non-vanishing couplings, this solution describes the vicinity of a multicritical point, in close analogy with the $O(2)$ model analysed in [43]. E.g. the tri-critical point represents microscopically the vertex model in presence of vacancies and dimers with negative fugacity.

The fact that the solution has different asymptotics at $x \rightarrow +\infty$ and $x \rightarrow -\infty$ marks an important difference between the gravitational vertex model and the other solved models of 2D QG. In the $O(2)$ model, which corresponds to $\lambda = 0$, the uniformisation map has the symmetry $s \rightarrow -s$. Because of this symmetry the parameters of the branch points must be at $s_{\text{b}}^{\pm} = \pm i\pi/2$ and the two infinite-order branch points at $\Re s \rightarrow \pm\infty$ can be identified. This \mathbb{Z}_2 symmetry is present also in the $O(n)$ model with $|n| < 2$ and in all generalised minimal models of 2D gravity, but not in the vertex models.

4.6 Computation of the boundary entropy

The parameter M can be determined as a function of the bare couplings κ and T by the exact solution before the continuum limit. Up to a numerical factor, this is the distance M_{b} of the support of the eigenvalue density from the origin of the x -plane. $M_{\text{b}}(\lambda, t)$ gives renormalised the boundary entropy of the sine-Gordon model on a fluctuating lattice which determines the exponential decay of the disk amplitude for given boundary length.

In the continuum limit, it is possible to determine the functional dependence of the parameter M on the renormalised couplings μ and t by substituting the solution (4.18) in the equations (4.4). We have

$$\varphi(s) = \int^s y(s') dx(s') = c_+ e^{2s} + c_- e^{-2s} + c_3 s + \text{const} \quad (4.20)$$

with

$$c_{\pm} = \frac{1}{2}(1 \mp \lambda) M^{\frac{2}{1 \mp \lambda}} \quad \text{and} \quad c_3 = (1 + \lambda) M^{\frac{2}{1-\lambda}} - (1 - \lambda) t M^{\frac{2}{1+\lambda}}. \quad (4.21)$$

In the parametrisation strip, the now infinite A -cycle connects the points $s = -\infty$ with $s = +\infty$, and the B -cycle connects the two edges of the s -parametrisation strip. The second relation (4.4) states, in terms of $\varphi(s) \equiv \varphi[x(s)]$, that for any s ,

$$S(s) \equiv \frac{\varphi(s + i\pi/2) - \varphi(s - i\pi/2)}{i} = 2\pi\mu. \quad (4.22)$$

Only the last term in (4.20) contributes to the difference and we arrive at the transcendental (for irrational λ) equation (1.7) for the boundary entropy $M = M(\mu, t)$,

$$\mu = \frac{1+\lambda}{2} M^{\frac{2}{1-\lambda}} - \frac{1-\lambda}{2} t M^{\frac{2}{1+\lambda}}. \quad (4.23)$$

This equation can be solved as a power series in t with finite radius of convergence,

$$\begin{aligned} M &= -\frac{1-\lambda}{2} \left(\frac{2\mu}{1+\lambda} \right)^{\frac{1-\lambda}{2}} \sum_{n=0}^{\infty} \frac{\Gamma\left(n\lambda(1-b^2) - \frac{b^2}{1+b^2}\right)}{\Gamma\left(\frac{1}{1+b^2} - nb^2\right)} \frac{(-\hat{t})^n}{n!} \\ &= \left(\frac{2\mu}{1+\lambda} \right)^{\frac{1-\lambda}{2}} (1 + (1-\lambda)\hat{t} + \dots) \end{aligned} \quad (4.24)$$

where \hat{t} denotes the dimensionless coupling

$$\hat{t} \equiv b^2(2\mu)^{-\frac{2\lambda}{1+\lambda}} t. \quad (4.25)$$

4.7 Partition function on the sphere and susceptibility

Now we will find the derivative of the partition function on the sphere from the first equation (4.4). The contour integral of $Y dx = d\varphi$ becomes, in the s -parametrisation, twice the linear integral along one of the two boundaries of the parametrisation strip,

$$\partial_\mu \mathcal{F}_0 = -\frac{2}{i} \int_{\Im s = \pi/2} y(s) dx(s). \quad (4.26)$$

It is easier to derive an equation for the second derivative $u = \partial_\mu^2 \mathcal{F}$ often called susceptibility. Let us first compute the derivative $\partial_\mu Y(x)$ using the s -parametrisation,

$$\partial_\mu Y(x) \equiv \partial_\mu y(s)|_x = \partial_\mu M \left(\frac{\partial y(s)}{\partial M} \Big|_s - \frac{\partial x(s)}{\partial M} \Big|_s \frac{y'(s)}{x'(s)} \right) = \frac{1}{x'(s)}. \quad (4.27)$$

This relation is in fact quite general and reflects the existence of a classical one-dimensional Hamiltonian system for which $x = x(s), y = y(s)$ define a classical phase-space trajectory, with $\varphi(s)$ being the abbreviated action. Since $\partial_\mu x = 0$, eq. (4.27) can be written in the form of Poisson bracket,

$$\{x, y\} = 1, \quad \text{with} \quad \{f, g\} \equiv \frac{\partial f}{\partial s} \frac{dg}{\partial \mu} - \frac{\partial g}{\partial s} \frac{df}{\partial \mu}. \quad (4.28)$$

Now we can obtain the derivative $\partial_\mu \varphi$ by integrating both sides of (4.27),

$$\partial_\mu \varphi(s)|_x = \int \partial_\mu [y(s)x'(s)]_x ds = \int \partial_\mu y(s)|_x x'(s) ds = s. \quad (4.29)$$

Since the A -cycle becomes infinite in the continuum limit, we regularise the integral (4.26) by introducing an UV cutoff Λ . Retaining only the leading term in the large x expansion, we have

$$u \equiv \partial_\mu^2 \mathcal{F}_0 = -2(\partial_\mu \varphi|_{x=\Lambda} - \partial_\mu \varphi|_{x=-\Lambda}) \approx -2 \left(\frac{1}{1-\lambda} + \frac{1}{1+\lambda} \right) \log(\Lambda/M) \approx -\frac{4}{1-\lambda^2} \log \frac{\Lambda}{M}. \quad (4.30)$$

Now we can substitute in (4.23)

$$M = e^{-\frac{1-\lambda^2}{4} u}. \quad (4.31)$$

from (4.30) to arrive at the equation (1.9) for the susceptibility,

$$\mu = \frac{1+\lambda}{2} e^{-\frac{1+\lambda}{2}u} - \frac{1-\lambda}{2} t e^{-\frac{1-\lambda}{2}u}. \quad (4.32)$$

The three critical points of this equation correspond to the expected three scaling regimes of the sine-Liouville gravity, $t = 0$, $t \rightarrow -\infty$ and $t = t_c > 0$. The third critical point is determined by $\partial\mu/\partial M|_{t=t_c} = 0$. In the vicinity of the three critical points the free energy is given by

$$\mathcal{F}_0 = \begin{cases} -\frac{1}{1+\lambda}\mu^2 \log \frac{2\mu}{1-\lambda} & (t \rightarrow 0), \\ -\frac{1}{1-\lambda}\mu^2 \log \frac{2\mu}{(1-\lambda)t} & (t \rightarrow -\infty) \\ -\text{const} \times (t_c - t)^{5/2} & (t \rightarrow t_c - 0). \end{cases} \quad (4.33)$$

Let us compare the curve (4.32) with what is expected from the world-sheet theory with $p = 1/\lambda$. Obviously the critical point $t = t_c$ is that of the pure gravity. Furthermore, the parameter t ranging from 0 to $-\infty$, (4.32) gives the evolution of the susceptibility along the massless flow connecting the critical and the low-temperature fixed points, both described by a compactified boson coupled to the Liouville field. The compactification radii at the two extremities of the flow extracted from the expressions (4.33) for the free energy are the inverse powers of $R_{\text{UV}} = \frac{1}{2}(1 + \lambda)$ and $R_{\text{IR}} = \frac{1}{2}(1 - \lambda)$ predicted by the world-sheet theory. This means that concerning the free energy, the continuum limit of the gas of oriented loops describes the fluctuations of the T-dual field $\tilde{\varphi}$.

The equation of state (4.32) has been derived previously in [12] in the context of MQM perturbed by a condensate of winding modes and its small t expansion reproduces the correlation functions of the sine-Liouville perturbation conjectured by Moore [1]. The large t expansion is then automatically obtained using the symmetry of the equation under

$$\mu \rightarrow \mu' = -\frac{\mu}{t}, \quad \lambda \rightarrow -\lambda. \quad (4.34)$$

The symmetry of the equation is compatible with the phase structure of the sine-Gordon model. The weak/strong coupling expansion describes a perturbation of a free boson compactified at $R = \frac{1}{2}(1 \pm \lambda)$ and coupled to Liouville gravity by a relevant/irrelevant sine-Liouville interaction.

Since μ_B scales as M , eq. (4.23) gives different scaling of the boundary length with the area both in the dense and in the dilute phases. In the dilute critical phase $\ell \sim A^{\frac{1-\lambda}{2}}$ and in the dense phase $\ell \sim A^{\frac{1+\lambda}{2}}$. Both scalings are anomalous for $\lambda > 0$ ($b < 1$) in contrast with the gravitational $O(n)$ model, where only the scaling in the dense phase is anomalous.

4.8 Boundary length distribution

In the scaling limit, the disk partition functions for fixed boundary constant x and for fixed boundary length ℓ are related by Laplace transformation,

$$W(x) = \int_0^\infty d\ell \tilde{W}(\ell) e^{-\ell x}, \quad \tilde{W}_\ell = \frac{1}{2\pi i} \int_\uparrow dx e^{\ell x} W(x), \quad (4.35)$$

where in the last integral the contour goes in the imaginary direction, to the right of the branch points. We cannot express the resolvent in a closed form, but from the second relation (4.2) which reads, for the inverse Laplace images,

$$\tilde{Y}(\ell) = \frac{1}{i} \left(\tilde{W}(q^{1/2}\ell) - \tilde{W}(q^{-1/2}\ell) \right), \quad (4.36)$$

we can reconstruct the small ℓ expansion of $\tilde{W}(\ell)$ from the inverse Laplace image of $Y(x)$. The integral can be expressed as a difference of two linear integrals by closing the contour around the two cuts of $Y(x)$. After partial integration,

$$\tilde{Y}(\ell) = \frac{1}{2\pi i} \int_{\uparrow}^{\infty} dx Y(x) e^{\ell x} = -\frac{1}{\ell} \Im \int_{-\infty}^{\infty} e^{\ell x(s+i\pi/2)} dy(s+i\pi/2). \quad (4.37)$$

Then $\tilde{W}(\ell)$ is reconstructed from (4.36) as

$$\tilde{W}(\ell) = \frac{1}{\ell} \int_{-\infty}^{\infty} e^{-\ell M(e^{-(1+\lambda)s} + e^{(1-\lambda)s})} d \left(M^{\frac{1+\lambda}{1-\lambda}} e^{-(1+\lambda)s} + t M^{\frac{1-\lambda}{1+\lambda}} e^{(1-\lambda)s} \right). \quad (4.38)$$

The integral (4.37) can be expressed in terms of a generalisation of the K-Bessel function which, as far as we know, has not been considered previously and which we denote by $K_{\nu}^{(b)}(z)$. For $\Re z > 0$, the function $K_{\nu}^{(b)}(z)$ is defined by the integral,

$$K_{\nu}^{(b)}(2z) = \frac{1}{2} \int_0^{\infty} e^{-z(\omega^{1/b} + \omega^{-b})} \omega^{\nu-1} d\omega, \quad \Re z > 0. \quad (4.39)$$

The function $K_{\nu}^{(b)}(z) = K_{-\nu}^{(1/b)}(z)$ satisfies the recursion relations

$$\begin{aligned} 2\partial_z K_{\nu}^{(b)}(z) &= -K_{\nu+1/b}^{(b)}(z) - K_{\nu-b}^{(b)}(z), \\ 2\nu K_{\nu}^{(b)}(z) &= b^{-1} z K_{\nu+1/b}^{(b)}(z) - b z K_{\nu-b}^{(b)}(z). \end{aligned} \quad (4.40)$$

and behaves for large positive argument as

$$K_{\nu}^{(b)}(2z) \sim \frac{e^{-zM_b}}{\sqrt{z}}, \quad (4.41)$$

where M_b is given by (4.11) with $2M = 1$.

Now, changing in eq. (4.37) the integration variable to $\omega = e^{-2s/(b+b^{-1})}$, we write the disk amplitude with marked boundary as

$$\tilde{W}(\ell) = \frac{1}{\ell} \left(bM^{b^2} K_b^{(b)}(2M\ell) - \frac{t}{b} M^{b-2} K_{1/b}^{(1/b)}(2M\ell) \right). \quad (4.42)$$

5 Relation to Matrix Quantum Mechanics and 2D string theory

5.1 The classical spectral curve of MQM

A non-perturbative formulation of the 2D bosonic string theory is provided by Matrix Quantum Mechanics (MQM) [8–11]. A standard review on the MQM approach is [44].

The idea is to discretise only the gravitational path integral as the ensemble of planar graphs embedded in a one-dimensional continuum, the MQM time. In the continuum limit, the singlet sector of MQM reduces to the dynamics of free fermions in inverted quadratic potential with a stabilising potential wall far from the top. In the grand canonical ensemble, the cosmological constant related to the Fermi energy, $\mu = E_F^{\max} - E_F$. The maximal value, near which the quantum effects become important, is convened to be zero. The thermodynamical limit corresponds to a Fermi sea filled up to Fermi energy $E_F = -\mu$ and sufficiently far from the maximum. In this regime the dynamics is that of a one-dimensional classical Hamiltonian system with $H = P^2 - X^2$. The individual particles follow classical phase-space trajectories $X = x(E, \tau), P = p(E, \tau)$. The profile of the Fermi sea of the unperturbed system is stationary and follows the trajectory of the particle with maximal energy $E = -\mu$, namely $\frac{1}{2}(X^2 - P^2) = \mu$, which also determines the classical spectral curve of the unperturbed MQM. The spectral density is proportional to the discontinuity of the function $P(X)$ on the cut $-\infty < X < \sqrt{2\mu}$,

$$\int_{H(P,X) \leq -\mu} dP \wedge dX = \int_{-\infty}^{-\sqrt{2\mu}} dX \rho(X), \quad \rho(X) = P(X) = \sqrt{X^2 - 2\mu}. \quad (5.1)$$

- *Integrable perturbations by momentum modes*

The MQM is known to be solvable in a nontrivial, time-dependent background generated by a finite tachyon source. Dijkgraaf, Moore and Plesser [14] showed that when the allowed momenta form a lattice as in the case of the compactified Euclidean theory, the perturbation exhibits Toda integrable structure. Toda integrability was exploited to investigate different aspects of the 2D bosonic string – winding mode [12] and momentum mode [13, 15, 45] condensates as well as non-perturbative effects due to sine-Liouville instantons [16, 17, 46]. The explicit construction of Toda flows with a constraint (string equation) is summarised in [31].

The Toda flows take simpler form in the chiral representation [13, 45]

$$X_{\pm} = \frac{X \pm P}{\sqrt{2}} \quad (5.2)$$

where the Hamiltonian $H = X_+ X_-$ is diagonalised by Fourier transformation. The sine-Liouville perturbation is then introduced by requiring that the wave functions behave at $X_{\pm} \rightarrow \infty$ as exponentials of $t_{\pm 1} X_{\pm}^{1/R}$. The grand partition function of the theory at finite temperature with $\beta = 2\pi R$ obeys, as a function of t_1, t_{-1} and μ , Toda equation which, together with the string equation, determines the susceptibility $\chi = \partial_{\mu}^2 \log \mathcal{F}_0$ in the thermodynamical limit through the equation of state

$$\mu = e^{-\chi/R} - \frac{1-R}{R} t_1 t_{-1} e^{-\frac{1-R}{R} \chi/R}, \quad R > R_{\text{BKT}} = 1/2. \quad (5.3)$$

The restriction $R > 1/2$ comes from the requirement that the perturbation is relevant. The deformed profile of the Fermi sea is the classical phase-space trajectory for $E = -\mu$,

$$X_{\pm} = x_{\pm}(\tau), \quad x_{\pm}(\tau) = e^{-\chi/2R} e^{\pm \tau} + t_{\mp 1} e^{-\frac{1-R}{R} \chi/2R} e^{\mp \frac{1-R}{R} \tau}. \quad (5.4)$$

For τ restricted to the real axis, this is a section of a complex curve where both variables X_+ and X_- are taken real. The spectral curve depends only on the product $t = t_1 t_{-1}$ because the dependence on t_1/t_{-1} can be eliminated by rescaling X_{\pm} . The spectral density $\rho(X)$ of the perturbed model is given in parametric form as $\rho \sim x_+(\tau) - x_-(\tau)$, $X \sim x_+(\tau) + x_-(\tau)$.

- *Integrable perturbations by winding modes*

The sine-Liouville perturbation in the T-dual theory is achieved by imposing $U(N)$ -twisted periodicity in the time which effectively introduces a condensate of winding modes [12, 47–50]. The perturbation is relevant for $R < \tilde{R}_{\text{BKT}} = 2$. The resulting integral over the eigenvalues of the twisting matrix, first obtained (for the non-perturbed theory) by Bulatov and Kazakov [51], resembles the eigenvalue integral (1.3), but with the unit circle as integration contour accompanied by a prescription for surrounding the poles.

The unitary matrix integral can be mapped to free fermions. In the unperturbed theory, the classical fermionic trajectories are given by a section of the complex curve $Z\bar{Z} = \mu$ where the variables Z and \bar{Z} are taken complex conjugated to each other.

Perturbations by winding modes also satisfy Toda hierarchy [12] and a string equation for which the Lax operators were constructed in [50]. The partition function $\mathcal{Z} = \exp(\mathcal{F}/\hbar^2)$ perturbed by a condensate of the two lowest winding modes with couplings t_1 and \bar{t}_1 satisfies Toda equation

$$\frac{\partial}{\partial t_1} \frac{\partial}{\partial \bar{t}_1} \mathcal{F}(\mu) + \exp\left(\frac{1}{\hbar^2} [\mathcal{F}(\mu + i\hbar) + \mathcal{F}(\mu - i\hbar) - 2\mathcal{F}(\mu)]\right) = 0 \quad (5.5)$$

with boundary condition for $t_1 \bar{t}_1 = 0$

$$\mathcal{F}(\mu) = -\frac{1}{2} R \mu^2 \log \mu - \hbar^2 \frac{R+R^{-1}}{24} \log \mu + \mathcal{O}(\hbar^2). \quad (5.6)$$

In the thermodynamical (dispersionless) limit $\hbar \rightarrow 0$, the solution for the susceptibility $\chi = \partial_{\mu}^2 \mathcal{F}$

$$\mu = e^{-\chi/R} - (R-1)t_1 \bar{t}_1 e^{(1-R)\chi/R}, \quad R < 2. \quad (5.7)$$

The classical fermionic phase-space trajectories are given in parametric form by $Z = z(\omega)$, $\bar{Z} = \bar{z}(\omega)$, where ω is a unimodular parameter and

$$\begin{aligned} z &= e^{-\frac{1}{2}\chi} \omega (1 + \bar{t}_1 e^{\frac{2-R}{2R}\chi} \omega^{-1})^R \\ \bar{z} &= e^{-\frac{1}{2}\chi} \omega^{-1} (1 + t_1 e^{\frac{2-R}{2R}\chi} \omega)^R. \end{aligned} \quad (5.8)$$

This spectral curve appears also in another realisation of MQM as a normal matrix model [52].

5.2 7vMM versus MQM

- *Condensate of momentum modes*

It is easy to see that the MQM with momentum-mode perturbation and the 7-vertex matrix model have the same spectral curve. By a linear change of the parameter, $s =$

$-\frac{\tau}{\lambda+1} - \frac{\lambda}{1-\lambda^2} \log(M)$, the spectral curve of the vertex matrix model, eq. (4.18), takes a form very similar to (5.4)

$$\begin{aligned} x(\tau) &= -e^\tau M^{\frac{1}{1-\lambda}} + e^{\frac{1-\lambda}{1+\lambda}\tau} M^{\frac{1}{1+\lambda}}, \\ y(\tau) &= e^\tau M^{\frac{1}{1-\lambda}} - t e^{\frac{1-\lambda}{1+\lambda}\tau} M^{\frac{1}{1+\lambda}}. \end{aligned} \tag{5.9}$$

The two curves become identical upon setting

$$\begin{aligned} X_+(\tau) &= y(\tau), \quad X_-(\tau) = -x(\tau), \quad t_{-1} = -1, \\ t_1 &= -t, \quad R = \frac{1}{2}(1 + \lambda), \quad e^\chi = M^{\frac{1+\lambda}{1-\lambda}}. \end{aligned} \tag{5.10}$$

Furthermore the equations of state (5.3) and (1.9) match if

$$\mu|_{7\text{vMM}} = R\mu|_{\text{MQM}}, \quad uR = \chi/R. \tag{5.11}$$

Integrating twice, we find that the free energies of the 7vMM and the MQM for $1/2 < R < 1$ are related by T-duality.

Expanding both sides of (5.11) in t , we conclude that the correlation functions of the thermal operator in the loop gas model and the correlation functions of the operator creating a pair of tachyons with momenta $p = \pm 1/R$ in MQM are the same. On the other hand, the boundary observables in the two theories are obviously different. For instance, in the MQM the dimension of the boundary is half of the dimension of the bulk while in the 7vMM, as we have seen, the dimension of the boundary is anomalous both in the dilute and in the dense phases.

The 7vMM describes the interval $\frac{1}{2} < R < 1$ while the MQM with a momentum mode condensate is defined for $\frac{1}{2} < R < \infty$. In the Minkowskian picture of MQM, both regimes $\frac{1}{2} < R < 1$ and regime $1 < R < \infty$ represent time-dependent backgrounds, with the correlation functions of exponential fields interpreted in terms of multiple scattering of massless tachyons off the ‘‘Liouville wall’’. However the physics in the two regimes is different. When $R > 1$, the two chiral sectors of incoming and outgoing tachyons decouple at infinity and the tachyon scattering is well defined. We have a ‘‘regular’’ background which can be interpreted in terms of multiple tachyon states reflected from a time dependent, but always time-like, Liouville wall. On the other hand, if $\frac{1}{2} < R < 1$, the Liouville wall becomes at some moment space-like and the outgoing tachyons can no longer be defined. In [53], see also [54], a quite involved picture was presented in which tachyons emitted by the accelerating Liouville wall get eventually absorbed by it.

It would be very interesting to understand how this intricate physics is perceived from the point of view of 6vM. In the end, the same branch cut which spoils the standard tachyon scattering interpretation appears as condensation of eigenvalues of the 6vMM. The fact that the spectral curve have two different singular points (the infinite points of the domains \mathbb{C}_+ and \mathbb{C}_-) suggests that the asymptotic space for the tachyon scattering should be a direct sum of two sectors and that the scattering matrix is not diagonal.

More specifically, the Liouville wave functions which are the bulk one-point functions in the ℓ -representation [55] and can be expressed in terms of the generalised K-Bessel function

(4.37). The scattering off the Liouville wall is encoded in the small- z expansion

$$\begin{aligned} K_\nu^{(b)}(2z) &= -\frac{1}{2} \sum_{n=0}^{\infty} C_n(\nu, b) z^{b\nu+(1+b^2)n} - \frac{1}{2} \sum_{n=0}^{\infty} C_n(-\nu, 1/b) z^{-\nu/b+(1+b^{-2})n} \\ &= \frac{1}{2} b \Gamma(-b\nu) z^{b\nu} + \frac{1}{2} \frac{\Gamma\left(\frac{\nu}{b}\right) z^{-\frac{\nu}{b}}}{b} + \dots, \quad C_n(\nu, b) = (-1)^n \frac{b \Gamma(-b^2 n - b\nu)}{n!}. \end{aligned} \quad (5.12)$$

The asymptotic space is a direct sum of two sectors labeled by the two compactification radii and related by a symmetry $b \rightarrow 1/b$, or in terms of the compactification radius, by $R_b = 1/(1+b^2) \rightarrow R_{1/b} = 1 - R_b$. For imaginary ν , the two lowest terms of the expansion represent incoming and outgoing particles belonging to different sectors of the asymptotic space. A first site, the momentum is not conserved by the scattering, but actually it is conserved because in the two sectors the boundary length depends differently on the constant Liouville mode, see the discussion after eq. (4.34):

$$\begin{aligned} \ell &= e^{\frac{1+\lambda}{2}\phi} = e^{b^{-1}\ell/(b+b^{-1})} && \text{(dense phase)} \\ \ell &= e^{\frac{1-\lambda}{2}\phi} = e^{b\ell/(b+b^{-1})} && \text{(dilute phase)}. \end{aligned} \quad (5.13)$$

◦ *Condensate of winding modes*

Now we turn to the case of perturbations by winding modes. The equation of state (5.7) becomes identical to the equation of state (4.32) in the 7vMM upon replacing

$$R \rightarrow \frac{2}{1+\lambda}, \quad \chi \rightarrow u, \quad t_1 \bar{t}_1 \rightarrow t \quad (1 < R < 2). \quad (5.14)$$

At this point we are obliged to comment on the strong coupling analysis of the equation of state (5.7) presented in [12]. This expansion is mathematically correct but we are not able to integrate it in the physical picture we propose. In [12], the critical point corresponding to infinitely large perturbation was obtained by simply setting $\mu = 0$ in (5.7). From the perspective of the analysis we present here, by doing that we miss the logarithm in μ and obtain only the uninteresting analytic in μ part of the free energy on the rhs of (4.33). Our analysis suggests that the correct procedure would be to use the symmetry $\mu'/R' = -\mu/(t_1 \bar{t}_1 R)$, $R' = R/(R-1)$, which converts the weak-coupling expansion into a strong-coupling one. This procedure, which is compatible with the intuition we got from the 6vMM, implies that the strong perturbation limit describes sine-Liouville interaction for a different radius in the interval $2 < R' < \infty$ which does not include the radius $R = 3/2$ where the equivalence with the cigar coset model is expected. We do not exclude that the prescription to achieve the pure sine-Liouville theory applied in [12] still make sense, but in a different physical context.

6 Discussion

In this paper we proposed a microscopic realisation of the sine-Liouville gravity based on a “dilute” vertex model on dynamical lattice which represents a one-parameter generalisation of the six-vertex model considered earlier. We extracted the phase diagram of the theory

from the classical spectral curve of the dual large- N matrix model and gave a QFT interpretation of the critical points, helped by the phase diagram of the sine-Gordon model on a flat surface. In particular, we identified the gravitational equivalent of the massless flow in the sine-Gordon model with imaginary coupling constant.

- As in any theory of 2D gravity, the phase structure is determined by the phase structure of the matter field on a flat surface. The Liouville direction of the target space is related to the length scale in the matter QFT. Varying the cosmological constant μ one can explore different scales. The behaviour at small/large μ of the free energy tell us about the IR/UV fixed points of the matter QFT, respectively. In the case of sine-Gordon matter in the repulsive regime $4\pi \leq \beta_{\text{SG}} < 8\pi$ considered here, the two non-trivial critical points are related by a massless flow parametrised by negative temperature coupling, $-\infty < t < 0$. The vicinity of $t = 0$ is described by a gaussian matter field compactified on a circle of radius $R_{\text{UV}} = R$ and perturbed by a relevant sine-Liouville term with $\beta_{\text{SG}}^2 = 4\pi/R_{\text{UV}}$. The vicinity of $t \rightarrow -\infty$ is described again by a gaussian matter field but compactified at a different radius $R_{\text{IR}} = 1 - R$ and perturbed by an irrelevant sine-Liouville term with $\beta_{\text{SG}}^2 = 4\pi/R_{\text{IR}}$.

- While the QFT description of the universal properties in the bulk is well understood, this is not so for the boundary phenomena. Microscopically the boundary condition for the disk partition function (4.42) is that of fixed height for the height model of section 3.1. For the moment we do not know how to formulate this boundary condition in the world-sheet theory except in the case $\lambda = 0$ where the vertex model is equivalent to the $O(2)$ model and the boundary condition is of FZZT [56, 57] type. One of the possible approaches to construct the world-sheet boundary theory is through the boundary ground ring [58]. The functional equations for the boundary correlators imposed by the boundary ground ring have a microscopic interpretation within the loop gas [59–61] and can be generalised to $\lambda > 0$ in a straightforward manner [27].

- Here we studied the near critical behaviour of the vertex model with a single thermal coupling coupled to the vacancies. This is the simplest of an infinite hierarchy of multicritical points. On the flat lattice, the multicritical phases of the vertex model are the same as the $O(n)$ loop model [62]. The multicritical phases and their microscopic construction for $\lambda = 0$ have been studied in [43].

- If we identify (up to a normalisation) the coupling constants $t_{\pm 1}$ in (5.3) with μ_{\pm} in the world-sheet action (2.9), the point $t_{\pm 1} = 0$ in MQM is described by a massless free boson coupled to Liouville gravity. On the other hand, in the 7vMM, $t_{-1} = 1$ even when $t = t_1 = 0$. This resembles the world-sheet description of the critical point $t = 0$ by a space-like Liouville field with $c = 25$ coupled to a time-like Liouville field with $c = 1$. Of course, the theories of 2D gravity with free boson and with the time-like Liouville as matter fields have the same set of bulk observables because of the charge conservation, but the two theories can have different boundary observables. In the unperturbed MQM, the boundary conditions are imposed independently on the Liouville field and on the free boson and hence of FZZT type. The boundary cosmological constant is coupled to the area of the

world sheet via the Liouville interaction $\mu_B e^\phi$. On the other hand, in the 7vMM, the disk partition function for $t \rightarrow 0$ is given by the first term on the rhs of (4.42) with $M \sim \mu^{(1-\lambda)/2}$ and certainly does not correspond to a FZZT brane. The only possibility is that boundary interaction in the world-sheet theory (2.9) involves both the Liouville and the matter fields. The simplest boundary term compatible with the scaling (5.13) is of sine-Liouville type,

$$\mu_+^B e^{(1-R)\phi} e^{iR\tilde{\varphi}} + \mu_-^B e^{(1-R)\phi} e^{-iR\tilde{\varphi}}, \quad (6.1)$$

where $\tilde{\varphi}$ is the T-dual field of φ , with $x \sim \mu_B = \mu_+^B \mu_-^B$. At the opposite end of the flow, where the gaussian field is perturbed by an irrelevant sine-Liouville operator, the boundary interaction with the correct scaling of the boundary parameter is again of the form (6.1), with $R \rightarrow 1 - R$.

◦ For $\lambda = 0$ ($q = -1$), Alexey Zamolodchikov conjectured [63] that Fredholm determinants of the type (3.8) solve the ‘‘TBA-like’’ integral equations which appear in certain $\mathcal{N} = 2$ supersymmetric theories [64] (see also [65]). This Zamolodchikov conjecture was later proved by Tracy and Widom [66]. The integral equations are better suited for numerical analysis than the differential equations from Toda hierarchy and it would be interesting to try to formulate them for general λ . The case $\lambda = 1/6$ was considered in [67].

Acknowledgments

I am grateful to Andre Alves Lima and Mateus da Silva Junca for numerous discussions, and Galen Sotkov for his interest and some important remarks. I thank Sergey Alexandrov, Vladimir Kazakov, David Kutasov and Valentina Petkova for providing useful comments on the draft version of the manuscript.

References

- [1] G. Moore, *Gravitational phase transitions and the sine-gordon model*, [hep-th/9203061](#).
- [2] E. Hsu and D. Kutasov, *The Gravitational Sine-Gordon model*, *Nucl. Phys. B* **396** (1993) 693 [[hep-th/9212023](#)].
- [3] V. Fateev, A. Zamolodchikov and A. Zamolodchikov, *unpublished*.
- [4] V.A. Fateev, *Integrable deformations of sine-liouville conformal field theory and duality*, *Symmetry, Integrability and Geometry: Methods and Applications* (2017) .
- [5] Y. Hikida and V. Schomerus, *The FZZ-duality conjecture — a proof*, *Journal of High Energy Physics* **2009** (2009) 095.
- [6] E. Witten, *String theory and black holes*, *Phys. Rev. D* **44** (1991) 314.
- [7] R. Dijkgraaf, H.L. Verlinde and E.P. Verlinde, *String propagation in a black hole geometry*, *Nucl. Phys. B* **371** (1992) 269.
- [8] V. Kazakov and A. Migdal, *Recent progress in the theory of noncritical strings*, *Nuclear Physics B* **311** (1988) 171.
- [9] E. Brezin, V.A. Kazakov and A.B. Zamolodchikov, *Scaling violations in a field theory of closed stringa in one physical dimension*, *Nucl. Phys.* **B338** (1990) 673.

- [10] P. Ginsparg and J. Zinn-Justin, *2d gravity+ 1d matter*, *Physics Letters B* **240** (1990) 333.
- [11] D. Gross and N. Miljkovic, *A nonperturbative solution of d= 1 string theory*, *Physics Letters B* **238** (1990) 217.
- [12] V. Kazakov, I. Kostov and D. Kutasov, *A matrix model for the two-dimensional black hole*, *Nucl. Phys.* **B622** (2002) 141 [[hep-th/0101011](#)].
- [13] S. Alexandrov, V. Kazakov and I. Kostov, *Time-dependent backgrounds of 2D string theory*, *Nucl. Phys.* **B640** (2002) 119 [[hep-th/0205079](#)].
- [14] R. Dijkgraaf, G. Moore and R. Plesser, *The partition function of 2d string theory*, *Nucl.Phys.* **B394** (1993) 356 [[hep-th/9208031](#)].
- [15] S. Alexandrov and V. Kazakov, *Correlators in 2D string theory with vortex condensation*, *Nucl. Phys.* **B610** (2001) 77 [[hep-th/0104094](#)].
- [16] S. Alexandrov and I. Kostov, *Time-dependent backgrounds of 2d string theory: Non-perturbative effects*, *JHEP* **0502** (2005) 023 [[hep-th/0412223](#)].
- [17] S. Alexandrov, R. Mahajan and A. Sen, *Instantons in sine-Liouville theory*, *Journal of High Energy Physics* **2024** (2024) 141 [[2311.04969](#)].
- [18] R. Baxter, *q colourings of the triangular lattice*, *Journal of Physics A: Mathematical and General* **19** (1986) 2821.
- [19] B. Nienhuis, *Critical behavior of two-dimensional spin models and charge asymmetry in the Coulomb gas*, *J. Stat. Phys.* **34** (1984) 731.
- [20] P. Fendley, H. Saleur and A.B. Zamolodchikov, *Massless flows. 1. The Sine-Gordon and O(n) models*, *Int. J. Mod. Phys.* **A8** (1993) 5717 [[hep-th/9304050](#)].
- [21] P. Fendley, H. Saleur and A.B. Zamolodchikov, *Massless flows, 2. The Exact S matrix approach*, *Int. J. Mod. Phys.* **A8** (1993) 5751 [[hep-th/9304051](#)].
- [22] A.B. Zamolodchikov, *Thermodynamics of imaginary coupled sine-Gordon: Dense polymer finite size scaling function*, *Phys. Lett.* **B335** (1994) 436.
- [23] I. Kostov, *O(n) vector model on a planar random surface: spectrum of anomalous dimensions*, *Mod. Phys. Lett.* **A4** (1989) 217.
- [24] P. Zinn-Justin, *The six-vertex model on random lattices*, *Europhys. Lett.* **50** (2000) 15 [[cond-mat/9909250](#)].
- [25] I. Kostov, *Exact solution of the six-vertex model on a random lattice*, *Nucl. Phys.* **B575** (2000) 513 [[hep-th/9911023](#)].
- [26] A. Elvey Price and P. Zinn-Justin, *The six-vertex model on random planar maps revisited*, *Journal of Combinatorial Theory, Series A* **196** (2023) 105739.
- [27] A.Alves Lima, I. Kostov and M.Da Silva Junca, *work in progress*.
- [28] V. Knizhnik, A. Polyakov and A. Zamolodchikov, *Fractal structure of 2d-quantum gravity*, *Mod. Phys. Lett.* **A3** (1988) 819.
- [29] F. David, *Conformal Field Theories Coupled to 2D Gravity in the Conformal Gauge*, *Mod. Phys. Lett.* **A3** (1988) 1651.
- [30] J. Distler and H. Kawai, *Conformal field theory and 2d quantum gravity*, *Nuclear Physics B* **321** (1989) 509.

- [31] I. Kostov, *Integrable flows in $c = 1$ string theory*, *J. Phys.* **A36** (2003) 3153 [[hep-th/0208034](#)].
- [32] J.V. José, L.P. Kadanoff, S. Kirkpatrick and D.R. Nelson, *Renormalization, vortices, and symmetry-breaking perturbations in the two-dimensional planar model*, *Phys. Rev. B* **16** (1977) 1217.
- [33] P. di Francesco, H. Saleur and J.B. Zuber, *Relations between the coulomb gas picture and conformal invariance of two-dimensional critical models*, *Journal of Statistical Physics* **49** (1987) 57.
- [34] P.H. Ginsparg, *Curiosities at $c = 1$* , *Nucl. Phys.* **B295** (1988) 153.
- [35] J.R. Hoppe, *Quantum Theory of a Massless Relativistic Surface and a Two-Dimensional Bound State Problem.*, Ph.D. thesis, Massachusetts Institute of Technology, Jan., 1982.
- [36] V. Kazakov, I. Kostov and N.A. Nekrasov, *D-particles, matrix integrals and KP hierarchy*, *Nucl. Phys.* **B557** (1999) 413 [[hep-th/9810035](#)].
- [37] J. Hoppe, V. Kazakov and I. Kostov, *Dimensionally reduced SYM(4) as solvable matrix quantum mechanics*, *Nucl. Phys.* **B571** (2000) 479 [[hep-th/9907058](#)].
- [38] R. Dijkgraaf and C. Vafa, *A perturbative window into non-perturbative physics*, [[hep-th/0208048](#)].
- [39] N. Dorey, T.J. Hollowood and S.P. Kumar, *S-duality of the leigh-strassler deformation via matrix models*, *Journal of High Energy Physics* **2002** (2002) 003.
- [40] M. Marino, *Spectral Theory and Mirror Symmetry*, *ArXiv e-prints* (2015) [[1506.07757](#)].
- [41] S. Zakany, *Matrix models and eigenfunctions from the Topological String/Spectral Theory correspondence*, Ph.D. thesis, éditeur non identifié, 2019.
- [42] M. Bousquet-Mélou and A.E. Price, *Refined enumeration of planar eulerian orientations*, *arXiv preprint arXiv:2503.15046* (2025) .
- [43] I. Kostov and M. Staudacher, *Multicritical phases of the $O(n)$ model on a random lattice*, *Nucl. Phys.* **B384** (1992) 459 [[hep-th/9203030](#)].
- [44] I.R. Klebanov, *String Theory in Two Dimensions*, *ArXiv High Energy Physics - Theory e-prints* (1991) [[arXiv:hep-th/9108019](#)].
- [45] S. Alexandrov, *Matrix quantum mechanics and two-dimensional string theory in non-trivial backgrounds*, 2003.
- [46] S. Alexandrov, V. Kazakov and D. Kutasov, *Non-perturbative effects in matrix models and D-branes*, *JHEP* **09** (2003) 057 [[hep-th/0306177](#)].
- [47] D.J. Gross and I.R. Klebanov, *Vortices and the nonsinglet sector of the $c = 1$ matrix model*, *Nucl. Phys.* **B354** (1991) 459.
- [48] V. Kazakov, *Vortex condensation and black hole in the matrix model of 2-d string theory*, [[hep-th/0105195](#)].
- [49] V. Kazakov, I. Kostov and D. Kutasov, *Matrix model of the (1+1) dimensional dilatonic black hole in the double scaling limit*, *JHEP proceedings, Non-perturbative Quantum Effects 2000 PoS(tmr2000)026* (2000) .
- [50] I. Kostov, *String equation for string theory on a circle*, *Nucl. Phys.* **B624** (2002) 146 [[hep-th/0107247](#)].

- [51] D. Boulatov and V. Kazakov, *One-dimensional string theory with vortices as the upside-down matrix oscillator*, *International Journal of Modern Physics A* **08** (1993) 809.
- [52] S. Alexandrov, V. Kazakov and I. Kostov, *2D string theory as normal matrix model*, *Nucl. Phys.* **B667** (2003) 90 [[hep-th/0302106](#)].
- [53] B. Balthazar, J. Chu and D. Kutasov, *On time-dependent backgrounds in 1+1 dimensional string theory*, 2023.
- [54] S. Das, S. Hampton and S. Liu, *Superluminal Liouville walls in 2d String Theory and space-like singularities*, [2509.12778](#).
- [55] G. Moore, N. Seiberg and M. Staudacher, *From loops to states in 2-D quantum gravity*, *Nucl. Phys.* **B362** (1991) 665.
- [56] V. Fateev, A.B. Zamolodchikov and A.B. Zamolodchikov, *Boundary Liouville field theory. I: Boundary state and boundary two-point function*, [hep-th/0001012](#).
- [57] J. Teschner, *Liouville theory revisited*, *Class.Quant.Grav.* **18** (2001) R153 [[hep-th/0104158](#)].
- [58] M. Bershadsky and D. Kutasov, *Scattering of open and closed strings in (1+1)-dimensions*, *Nucl. Phys. B* **382** (1992) 213 [[hep-th/9204049](#)].
- [59] I. Kostov, *Boundary correlators in 2d quantum gravity: Liouville versus discrete approach*, *Nucl.Phys.* **B658** (2003) 397 [[hep-th/0212194](#)].
- [60] I. Kostov, *Boundary ground ring in 2D string theory*, *Nucl. Phys.* **B689** (2004) 3 [[hep-th/0312301](#)].
- [61] I. Kostov, “Boundary ground ring and disc correlation functions in Liouville quantum gravity.” “Lie theory and its applications in physics - 5”, June 2003, Varna, Bulgaria, 2004.
- [62] A.B. Zamolodchikov, *Conformal Symmetry and Multicritical Points in Two- Dimensional Quantum Field Theory. (In Russian)*, *Sov. J. Nucl. Phys.* **44** (1986) 529.
- [63] A.B. Zamolodchikov, *Painleve III and 2-d polymers*, *Nucl. Phys.* **B432** (1994) 427 [[hep-th/9409108](#)].
- [64] S. Cecotti, P. Fendley, K.A. Intriligator and C. Vafa, *A New supersymmetric index*, *Nucl.Phys.* **B386** (1992) 405 [[hep-th/9204102](#)].
- [65] S. Cecotti and C. Vafa, *Topological antitopological fusion*, *Nucl.Phys.* **B367** (1991) 359.
- [66] C.A. Tracy and H. Widom, *Proofs of Two Conjectures Related to the Thermodynamic Bethe Ansatz*, in *eprint arXiv:solv-int/9509003*, p. 9003, Sept., 1995.
- [67] K. Okuyama and S. Zakany, *TBA-like integral equations from quantized mirror curves*, *JHEP* **03** (2016) 101 [[1512.06904](#)].